Authors Version

Integrated testing approach using a customized micro turbine for a volcanic ash and CMAS related degradation study of thermal barrier coatings.

R. Naraparaju, H. Lau[4], M. Lange, C. Fischer, D. Kramer U. Schulz and K. Weber

Surface & Coatings Technology

https://doi.org/10.1016/j.surfcoat.2018.01.30

Integrated testing approach using a customized micro turbine for a volcanic ash and CMAS related degradation study of thermal barrier coatings.

R. Naraparaju[1]*, H. Lau[1, 4], M. Lange[2], C. Fischer[2], D. Kramer[3], U. Schulz[1] and K. Weber[2]

[1]Institute of Materials Research, German Aerospace Centre, Köln, Germany

[2]University of Applied Sciences, Duesseldorf, Germany

[3]Hammer engines Gmbh, Henfenfeld, Germany

[4] Lloyd's Register EMEA, Hamburg, Germany

Abstract:

A volcanic ash (VA) test stand has been built with a precise particle feeder, concentration measuring unit and a mini turbine with an integrated thermal barrier coating (TBC) system on the blisk for the first time in a laboratory scale. This setup has allowed the testing of melting, sticking, corrosion and erosion behaviour of volcanic ash in-situ at high temperature in a realistic manner in a gas turbine. Moreover, this mini engine runs with kerosene which could also bring all the impurities such as sulphur in to system which might change the reaction mechanisms of TBC and VA. The particle size influence on the sticking/escape behaviour in the engine components was tested but a clear statement on the particle size versus its sticking behaviour could not be made, although the particles in the size range of 1-10 µm are more susceptible to melting in the given conditions. The blisks were coated with two different TBC materials such as 7 wt.% Yttria Stabilised Zirconia (7YSZ) and Gadolinium Zirconate (GZO) using Electron Beam Physical Vapour Deposition (EB-PVD) technique. Both coatings were tested in corrosion-erosion regime under VA at high temperature and it was found out that the coating with higher toughness (7YSZ) has performed better than the other coating under the used testing conditions.

Keywords: Volcanic ash, CMAS, TBCs, Turbine blisk, GZO, 7YSZ.

1. Introduction

Ever since the Eyjafjallajökull volcano in Iceland erupted in 2010 which has caused a major shut down of European aerospace, the threat from volcanic ash to aviation has been widely recognised [1-6]. Volcanic ash (VA), can be ingested into jet engines and at higher temperatures adhere to the internal components of the engine causing substantial damage [7-9]. In general each engine does normally contain three functional areas named as compressor, combustion and turbine. The temperature distribution among these areas varies from 100-1600°C depending upon the place of interest. The areas which exceed more than 1000°C in temperature contain metallic parts with functional ceramic coatings on top called Thermal barrier coatings (TBCs) [10]. These ceramic coatings are highly porous and have a very low thermal conductivity and hence they cause a temperature drop through them allowing the metallic parts operate at lower temperatures. In addition to the internal cooling within the metallic parts, these TBCs act as thermal insulators. Because of the relatively lower melting (<1100°C) point than the other sand like particles the thermal hazard from the VA adhesion is

high at the elevated temperature of the jet engine (1200-1400°C). With increasing turbine inlet temperatures (TIT) VA melts and infiltrates/reacts with the thermal barrier coatings and these TBC materials will lose their strain tolerance and sometimes will be peeled off and the underlying metallic parts are exposed to high temperatures and may damage during service which causes the shorter life time or shorter maintenance interval of the total engine/aeroplane [11]. According to Rolls-Royce 'Safe-to-Fly chart' which was constructed on the basis of reviewing the relevant gas turbine engine data which in past encountered the VA cloud, ash concentration of 2 mg/cm^3 was set as the safe limit to fly for the aviation engines [12]. Even though the interaction of molten VA with 7 YSZ TBCs is in principle clear, the deposition and the sticking mechanism of the VA particles on the turbine blade are unclear. i.e. whether the VA particles soften and melt within the combustor chamber and deposit on the turbine blade as a droplet or will they first adhere to the turbine blade and then melt because of the heat on the blade? What is the probability of a big VA particle to pass through the engine without being deposited on the blade etc. Of course it will also depend on the kinetic effects such as resident time of VA within the combustion and turbine sections which depends on type of the aero-engine since melting and sticking of VA would be influenced by time-at-temperature. Few attempts were made in understanding this criterion by injecting the VA powder with the size range of 10-70 µm into a modified vacuum plasma spray set-up on a rotatable stainless steel substrate and found out that particle sizes in the range of 10-30 µm are most likely to adhere [13]. In another such study from model experiments to determine the adhesion characteristics of several volcanic ashes on flat substrates, they found out that the tendency of adherence is high in low SiO_2 containing ashes [14]. However, the diversity in chemical composition among volcanoes worldwide results in varied melting conditions and rheological responses [15, 16]. Due to these differences, the melting behaviour of different volcanic ashes alters significantly with respect to temperature and hence their viscosity is changed accordingly. With all these unknown factors which influence the overall engine performance under volcanic ash attack, there exists a necessity to understand the relation of particle size to the flying behaviour through the turbine, particle size to the sticking/melting behaviour and the critical concentration of VA et al. which can cause a substantial damage to the blade. Experiments such as burner rig, laser rig and furnace cycle tests were performed to understand the chemical attack, infiltration depth and the lifetime assessment of different TBC materials [17-19]. Few techniques such as burner rig or laser rig tests are able to establish a thermal gradient (with back side cooling) within the TBC layer to simulate a realistic thermal condition of the layer as in a real turbine blade. However, very few efforts were carried out in-situ with a running engine under VA attack to estimate and understand the damage scenarios. The biggest recent effort is the NASA-led Vehicle Integrated Propulsion Research programme in which a Pratt & Whitney PW2000 engine on a Boeing C-17 airlifter on the ground but on wing is tested to simulate prolonged flight through a VA cloud [20]. Another lab scale effort has been made by Maya Shinozaki to simulate the realistic conditions by sending VA into a small gas turbine, thereby observing their sticking properties with respect to their size [21]. They have found significant deposits on the stationary surfaces such as nozzle guide vanes and adjoining blade platform but not on the blades. However, no laboratory experiments so far were conducted on TBC coated blades in a turbine to attain a deep insight to this problem.

A very first experiment of such kind, its design and execution is presented in this study. In addition, initial results of the test run conducted with Eyjafjallajökull ash are presented in this paper.

2. Experimental setup

The uniqueness of this experiment lies on the idea to send real VA particles through a mini turbine (which runs by kerosene which is used also in large aero-engines) coupled with a particle analyser shown schematically in Fig. 1.

With the help of a disperser (1) volcanic ash could be precisely injected in to a flow channel (2). The flow in the channel is driven by the turbine (4) (Hammer engines Gmbh, Henfenfeld) at a speed of 30 m/s at maximum thrust. The aerosol concentration in the intake air is measured with an iso-kinetic sampling (3) that is connected to an optical particle counter (OPC 1.109, company Grimm). The particle disperser in combination with the OPC allows to precisely tune the particle concentration in the intake air for example to 2 mg/m^3 or 4 mg/m^3. Using the OPC, the particle size distribution and the particle mass concentration can be determined. The OPC detects and counts aerosols with a size of 250 nm up to 32 µm by using scattered light measurement with a time resolution of 6 seconds. The particles are classified in 31 different sized channels having a size range from 0.25 to 32 µm. From the obtained number distribution, the mass concentrations can be calculated.

The mini turbine (4) has a single stage compressor section, a combustor chamber (which can reach up to 1600°C gas temperature), a vane section and the rotating bladed disk manufactured from IN713LC. The combustor chamber is 10 cm long and it is divided into two sections in which the first 7 cm belongs to the hot zone where a VA particle enters with a velocity of 13 m/s and accelerates linearly up to 150 m/s. Second part is the colder section where the particle accelerates up to 200 m/s. This disc is attached to a rotating shaft which is internally cooled with air. With TBC on top and cooling through conduction (blade to the shaft), a thermal gradient is established within the TBC similar to that of a real turbine blade. In addition to the described experimental set up, one thermocouple is installed in the combustor chamber to measure the exact temperatures in the chamber. Another two thermocouples could be installed near the blades and in the exhaust. With these temperature sensors, a complete thermal history of the gas flow including VA throughout the turbine can be monitored.

For the blades on the disk, a coating system consisting of a bond coat and a ceramic top coat was developed. The parts were coated with a 40 µm thick oxidation protective NiCoCrAlY bond coat (BC) using EB-PVD technique. Two TBC topcoats, 7YSZ and Gadolinium Zirconate GZO were tested against VA in this study. A TBC coating thickness of ~150 µm was achieved by means of EB-PVD technique. Real Eyjafjallajökull ash was collected at 63°40'42.10"N; 19°37'31.75"W about 4 km from the source. The particles were mechanically ground and sieved to two different size ranges 1-40 µm and 1- 10 µm were used to reproduce the characteristic size distribution of VA particles in a real volcanic ash plume and to optimize the OPC system. The melting behaviour of this ash was studied by means of Differential Scanning Calorimetry (DSC) using platinum crucible and a heating rate of 10 K/min. The

chemical composition of the VA used is given in Table 1. It can be seen from the table that the VA is rich in silica. These values are the average of 5 different energy dispersive X-ray detector (EDS) point measurements. To know the crystal nature of the VA particles a Siemens D5000 diffractometer using Cu-Kα radiation with a secondary graphite monochromator was used for standard x-ray diffraction analysis (XRD). VA was heat treated in a standard lab furnace at 1250°C for 10h and cooled down with a rate of 10°C/min. In another attempt VA was heated first to 1250°C for 10h and then air quenched. Later the molten VA was mechanically ground into a powder form and XRD measurements were carried on to know the crystal nature after complete melting.

The turbine was operated for 60 mins with the ash. After the test run, the bladed disk was dismantled from the engine and investigated using secondary electron microscope SEM and EDS. When VA is injected to the combustion chamber, it can melt in the combustion chamber providing that the engine runs at a temperature above the melting point of the specific ash. It is then blown on to the turbine components. The particles which did not encounter the blade will follow the exhaust gases and come out through the nozzle. In order to investigate these particles, they were trapped with a cooled, iso-kinetic sampling (5) and directed to an OPC. Since the OPC is very sensitive to opening of the iso-kinetic sampling nozzle, velocity of the particle and moisture in the exhaust, the measurements were done in special calibration runs while in the main VA experiments un-exposed turbine components have been used. Since the powder feeder is quite stable and feeding rates are repeatable, well defined VA concentrations could be achieved in the experiments.

Particles can also be collected by placing a particle collector instead of the OPC in the exhaust. The collected VA particles were investigated under SEM. Their chemical composition was analysed with an EDS detector. A likely morphology of the particles before entry into the combustion chamber is shown in Fig. 1 as an inset (a). When these particles melt in the combustion chamber they become spherical as shown as (b).

3. Results

3.1. Volcanic ash particle morphology, melting behaviour, crystallinity and dosage

Volcanic ash in the size range of 1-40 µm was used in all the runs that used the blisks for the deposition experiments. This fraction was chosen to test the influence of their size on the melting behaviour during their flight in the combustion chamber. Moreover, it represents the typical particle sizes found in volcanic ash clouds [3]. Fig. 2 shows the SEM morphology of the VA particles used in this study. Since they have sharp edges, it is likely that they can cause erosion damage to the parts. The DSC curve in Fig. 3 (a) shows the melting behaviour of the VA. The Eyjafjallajökull VA has a broad melting range of 1040-1200°C. That means, if the temperature of the combustion chamber rises to the upper boundary of the melting range, the VA particles can melt in their flight through the chamber. XRD results (See Fig. 3(b)) show that the used VA is mainly amorphous in nature. After annealing and slow cooling it crystalizes to (Fe, Ti) oxide where as a quick air quenching resulted in much smaller presence of (Fe,Ti) oxide in addition to the pure glass. These results indicate that this VA ash needs

longer annealing times in order to crystalize. It can be assumed that they are in a glassy state in the current scenario as the particle flight time in the hot zones will be barely in fraction of a second.

In order to optimize the OPC sensitivity towards the smaller particles, VA in the size range of 1-10 µm were used at first. The disperser settings were stepwise changed to increase the concentration of volcanic ash (level 0 – level 6) and the corresponding particle measurements were performed by the OPC in front of the turbine, see Fig. 4. These tests were run several times using different dosages and sensitivity of the OPC was optimised. Fig. 4(a) shows the particle size distribution and Fig. 4(b) shows the concentration of injected VA measured by OPC in one of such runs. The maximum number of VA particles lies in the size range of 0.5-7 µm (for all the disperser settings which matched with the SEM measurements) and the minimum VA concentration of 4 mg/m^3 could be achieved with a disperser setting of '0'. By changing the disperser settings to 1, 2, 3 and 6 VA concentrations of 6, 8, 12 and 20 mg/m^3 could be achieved. i.e. precise VA feed rate could be achieved with the calibrated disperser with the optimized sensitivity of the OPC to detect the smaller particles.

3.2.Microstructure of the coating

The particular geometry of the bladed disk that needed to be coated is shown in Fig. 5. The non-masked area is the one that is exposed to the hot airflow which needs to be protected. Note that the profile in the center of the blade is covered with a filling in order to protect the company's know how on such blisk profiles. Coating such kind of a disk was itself a challenging task for all non-line-of sight techniques such as EB-PVD (because each blade shadows the other blade). First a NiCoCrAlY bond coat at a thickness of around 40 µm with some variation in thickness across the blade was coated. Then the coated blisks were shot-peened and subsequently annealed at 1080°C in vacuum for 4 h. This treatment was done to densify the EB-PVD bond coat prior to the 7YSZ and GZO TBC deposition. Fig. 5 shows the un-coated (left) and a coated (right) disk for comparison. It is extremely difficult to apply a TBC of sufficient uniform thickness and of desired porosity on such a bladed disk. Therefore, much attention was paid to an appropriate movement pattern of the parts during EB-PVD deposition. Cross sections of the coating along a blade are shown in Fig. 6.

The thickness over different positions of the blade varied to some extent but the thickness was higher than 110 µm in all areas of the blade. Higher thicknesses were noticed at the leading and trailing edges and this is due to the fact that those positions of the blade face directly to the vapour pool during the EB-PVD process and did not suffer much from shadowing. Moreover, the morphology of the coating at different locations seems to vary very little, as shown in Fig. 6.

3.3.Test run

(a) Bond coated blisk

A trail run was conducted to examine the functionality of all units including disperser, OPCs, mini turbine and temperature sensors. Eyjafjallajökull ash (size 1-40 µm) was used in this run

and a bond coated-only blisk was installed in the engine. The ash feed rate was changed several times during the 1 h test run. The gas temperature in the combustor chamber was measured as high as 1450°C at 90% of the total engine power (suction capacity of 27 m/s). Based on the combustion chamber dimensions and the thrust created by the engine few calculations were made on the velocities of the VA particles in the chamber. Avoiding the turbulent flows, volcanic ash particle enters with an initial velocity of 13 m/s in the chamber and linearly accelerates up to 150 m/s in the hot section and even it reaches up to 200m/s in the cold section of the combustion chamber. Based on the velocities the time that particle stays within the combustion chamber is around 0.9 ms. Volcanic ash particles were collected in the exhaust and were examined in SEM. The corresponding micrographs are presented in Fig. 7. It is immediately apparent from Fig. 7(a) that the collected pool of particles contain both molten (spherical) and unmolten (with sharp edges) VA. i.e. few particles were not molten during their flight path as an effect of their size, heat capacity and flight time. The average size of these un-molten particles was found to be greater than 12 µm. Diameters of the molten spherical particles were found to be in the range of 0.5-10 µm. A high magnification micrograph of the molten spherical particle is shown in Fig. 7(b). The engine inspection after the first run revealed that most of the colder parts such as compressor blade were heavily eroded. High amount of molten/semi molten VA was accumulated in the combustion chamber. Later the turbine was dismantled and the turbine blisk was dismounted for the examination. Blades were considerably eroded and VA deposition on the blades could be observed as shown in Fig. 8. Ample spallation of bond coat was observed on few places of the blade.

SEM cross-sectional analysis of one of the blades is presented in Fig. 9. In general the leading edge of the blade has substantially more deposit than the trailing edge. VA deposition on the leading edge is illustrated by the micrograph shown in Fig. 9(a). The corresponding higher magnification SEM back scattered electron (BSE) image is shown in Fig. 9(b). A difference in the physical appearance of VA deposit between the suction and pressure sides of the blade is quite evident from the Fig. 9(c)&(d). On the suction side VA looks more molten and on the pressure sides it is in semi molten state and more porous which resembles the deposition in real aviation engines as the temperature on the pressure side would be little colder than that of the suction side. The accumulated area of VA deposition on the suction side was found to be smaller than that of the pressure side. EDS elemental mapping (which is not shown here) on this layer confirmed the presence of Si, Ca, Al, Na, Ti and Fe.

(b) Blade with bond coat + 7YSZ coating

To understand the sticking/infiltration behaviour of VA on the state of the art TBC material a 7YSZ coated blisk was mounted in the engine. Volcanic ash (20 mg/cm^3) was injected into the mini turbine operated at full power for 60 min (combustion temperature nearly 1500°C and suction capacity of 30 m/s). The intention for using such a high dose of volcanic ash is to investigate the highest possible damage to the 7YSZ layer. Fig. 10 shows the photographs of the blisk before and after the test run including VA deposition.

From the very first macroscopic examination on the pressure sides it became clear that the blades had undergone severe erosion attack due to the impingement of the VA particles. The

dark colour on the pressure side of the blades represents the VA deposition and bright colour on the suction side assures the presence of 7YSZ coating. Higher deposition of VA was observed on the leading edge of the blade on the suction side and similar to that of only bond coated blade. The leading edge on the pressure side was predominated by erosion. The 7YSZ blade was cut and investigated under SEM. SEM cross sectional images of pressure side and suction side of the blade are given in Fig. 11. Erosion damage of the 7YSZ layer on the suction side can be noticed from Fig. 11(b). Very sharp ends of the broken columns represent the erosion attack. VA deposits can be seen on top of the TBC layer but VA infiltration related damage was not observed in the entire blade. However, the TBC is still intact on the blade, but its thickness is reduced in varying amounts depending on the location. Heavy reduction in the TBC thickness due to erosion was seen on the suction side of the blade compared to the pressure side. Uniform accumulation of VA deposit was observed on the pressure side compared to the suction side, and there was no indication for erosion on the pressure side except on the leading edge. These findings clearly indicate that the molten volcanic ash has been deposited on the coating but could cause neither a chemical attack nor infiltration in the TBC under the experimental conditions chosen for this test.

(C) Blade with bond coat + GZO coating

Another test run was performed by replacing the 7YSZ with the GZO coated blisk for exactly one hour with full power (with the same VA concentration and particle sizes of 1-40 µm as in the case of 7YSZ). GZO is known for its better infiltration resistance against VA/CMAS. From the macroscopic investigation of the blade given in Fig. 12 it was evident that VA deposition on the suction side was spread on a larger area compared to 7YSZ blades (see Fig. 10 &11, higher dark colour area on the blades). The SEM cross-sectional micrographs of the pressure and suction side of the GZO blade are shown in Fig. 13. On the suction side of the blade complete removal of GZO coating took place as shown in Fig. 13 (a) and (b). No VA infiltration or chemical reaction with GZO layer was observed similar to the 7YSZ blade. However, a lot of TBC has been removed as a result of erosion and the metallic bond coat was directly exposed to the VA on the suction side as shown in Fig. 13 (a). This is the reason for the presence of larger darker area on the suction side of GZO blades. VA deposit on the bond coat can be found on the Fig. 13 (b). i.e. during the 1 h exposure time, re-deposition of VA on the suction side took place after complete TBC removal. The TBC damage on the pressure side was not as high as on the suction side as shown in Fig. 13 (c)&(d). Higher amount of TBC removal was observed on the blade tips compared to that of 7YSZ blades.

4. Discussion:

The development of a test set up which was designed to determine the response of the TBC system to degradation by major constituents of volcanic ash which may present the worst case scenario for environmental attack is presented in this paper. The main goal was to evaluate how two different TBCs deposited on a bladed disk get influenced by volcanic ash that was partially melted in a real combustion chamber (maximum temperature of 1600°C). It is well known in the field of volcanology that the chemical composition of the VA erupted from the same volcano changes over the time period of the eruption. Therefore, it is very important to know the melting range of the VA (measured as 1040°C-1200°C using DSC) which was

collected from the site in Iceland after few days of eruption. Ultimately this set up was designed to answer the yet unknown but important questions such as the effects of VA particle size and its chemical composition, combustor chamber temperature and the TBC surface temperature on the VA interaction with TBCs and give a breakthrough in understanding the VA deposition/reaction mechanism with TBCs and its relation to erosion of the ceramic layers. The key findings from the present experimental set up can be postulated as following.

- From the literature it is known that the efficient particle size reduction of different VA/CMAS in the turbine compressor section leads to a typical particle size of 6 µm with significant amounts below 4 µm [12]. The present set up of the test apparatus can clearly detect those particles which are in this size and concentration range. Another study revealed that the particles less than 3 µm would flow around obstacles rather hitting them and the particles in the range of 10-30 µm are most likely to adhere [13]. In this study, microscopic inspection of the collected particles (see Fig. 7) in the exhaust reveals that most of the molten spherical particles are present in the size range from 1-10 µm. The larger particles (15-40 µm) were found to be either in semi molten or unmolten state. The measured combustor temperature of 1500°C surely assures the melting of VA particles (melting range is in between 1040°C-1200°C, see Fig. 3(a)) even though the particle stay time in the chamber is 0.9 ms). From this study it is evident that the probability of larger particles to melt in the flight path is lower compared to the smaller particles, which is mainly caused by the small dimension of the mini gas turbine and the short heating intervals of the ash particles. However, it is shown in the literature that the sticking behaviour does not depend on the full melting of the volcanic ash and softening of the VA is sufficient for sticking. This point lies in the very beginning of the melting process and this temperature is enough that VA particles stick to the material[16]. Even the bigger particle that do not completely melt, have probability of sticking to the TBCs. On the other hand, the gas flow velocity in the current test apparatus is much smaller than in larger aero-engines, giving more time for heat intake and melting of particles which countervail the effect of the small size of the turbine. It can be hypothesized that the plausibility for a particle to hit the blade is independent of its size (within the tested size range of 1-40 µm) with a rotating blade in action. This statement can be a little different from the previous studies because of several factors such as nature of volcanic ash, temperature of the gas flow and experimental set up. It was recently shown that the probability for the VA with low Si and significant content of Ca, Fe and Mg to adhere on the surfaces is much higher [14]. In another study with a little different experimental setup by sending VA in a rapid flowing acetylene-oxygen micro torch flame which accelerates the particles towards a Inconel 713LC (same blade material is used in this study), it was found out that bulk/glass volcanic ash compositions and grain size control the interaction with turbine blades [22]. A conclusive statement on the effect of particle size on the sticking nature could not be made directly but it is clear that “chemical composition of the VA which defines the viscosity and surface temperature of the TBC are the key factors for its sticking behaviour”. While the experimental setup in [11, 19] is able to reveal precisely the sticking behaviour on a flat surface, the current

test apparatus provides also information on the behaviour of volcanic ash in a real (mini) gas turbine within an accelerated stream of combustion gases.

- The ash concentration has an important significance in the diagram given by Rory Clarkson's for ash concentration vs. duration of engine exposure [12]. The overall engine degradation should be monitored on the basis of an accumulation factor rather than only ash concentration or size of the particle. Accumulation time with particular concentration of VA intake for an exact type of VA should be defined for 'Safe-to-fly' chart [12]. The allowable test range of the present set up with respect to VA concentration range and operating time is superimposed with the 'Safe-to-fly' chart and is presented in Fig. 14. The black box represents the operating window of the test apparatus where VA within the concentration range of 2-20 mg/m^3 can be blown in to engine and tested from 10 min to 5 h time regime. Note that the testing capability is limited with the higher concentration of VA as it could cause engine damage. The current experimental conditions which were used in this study are plotted as a red spot (slightly above 20 mg/m^3) within the black box which lies in the zone where 'long term damage' could happen to the engine similar to that of 'Hekla 2000 NASA event' and 'Kelut 2014'[23, 24]. In both these events it was noticed that the consequences were long-term damage to the engines such that they had to be prematurely removed from the aircraft shortly after exposure. However, the boundary of the long term damage region to the unsafe operation is currently unclear. More experiments with different VA types and doses need to be done to define the lower and upper limit of this boundary. With the present experimental set up it is possible to obtain accumulation factors and define the boundary between long term damage/unsafe operation zone with respect to the functionality of the TBCs for different initial conditions.

- This experimental set up adds valuable information in the chain of VA/CMAS related laboratory experimental research. There has been fundamental research using sophisticated high temperature imaging of the VA melting process, CFD modelling of the thermal and velocity fields of the gases to predict the VA particle velocity in the gas stream and flying/sticking behaviour of VA on a metal substrate [13-15, 21, 22]. Concurrently, several TBC testing methods have been developed to study the chemical interactions and life times of TBCs against VA namely furnace cycle tests, and thermal gradient tests [17-19, 25]. However, none of those methods could simulate real time damage caused by VA of the engine hardware and TBCs as several physical/chemical phenomenon operate together in an engine at the same time [26]. This set up enables to study the complete test cycle beginning from the VA deposition to the failure mechanism of the TBC coating which simultaneously could simulate the erosion, Foreign Object Damage (FOD), oxidation, and volcanic ash infiltration assisted TBC damage.

A typical reaction of VA with EB-PVD 7YSZ layer at high temperature was studied by Mechnich et al. systematically by using sol gel based artificial volcanic ash (AVA) matching the bulk composition of the April 15, 2010 Eyjafjallajokull at different temperatures. According to their study, at 1100°C AVA starts to cover the 7YSZ coating

with a dense glaze-like overlay and at 1200°C AVA was mostly infiltrating the coating [27]. Moreover, the reaction between AVA and 7YSZ yielded a new phase $ZrSiO_4$ as a by-product. However, such kind of infiltration or reaction could not be observed on both the 7YSZ layer and GZO in this study. Instead few interesting observations were made such as

- VA deposition has been observed on the 7YSZ coated blade and especially more deposits were found on the leading edge (see Fig.10). This deposition tendency was seen in the literature where a leading edge had substantially more CMAS deposit than the trailing edge of a HPT blade [28]. This behaviour could be explained on the basis of probable higher gas flow temperature on the leading edge than on the trailing edge, and the gas flow paths of particles through two neighbouring blades
- No infiltration of VA within the 7YSZ columns means that even though the particle temperature on impact is important and particles were partly molten as evidenced by spherical particles collected in the exhaust (see. Fig.7), the TBC temperature is equally important for the infiltration and reaction. Due to the lack of internal cooling of the blisk, it was needed to be operated at lower than 1100°C. It is assumed that the TBC was not hot enough to make the molten VA to flow and infiltrate. Infiltration in TBC regions that have spalled or eroded cannot be fully ruled out, but this only speculative.
- High erosion damage has been observed due to the sharp morphology of the VA particles as shown in Fig. 5. It was already shown in the literature that volcanic ash can be four times more erosive than sand on metallic coatings [29]. Especially Eyjafyallajokull ash was found to be up to 40% more erosive than the other real VA encounters, depending on the incidence angle [12]. One more such study by T.Uihlein et al. revealed that VA is more erosive on metallic parts than sand, and the extent of erosion can be correlated with their morphology. However such data is missing on TBC/VA erosion [30], but it is very likely that erosion of TBC is also higher by volcanic ash compared to sand The VA particles which flew through the combustor chamber without being molten still possibly cause this erosion damage. The erosion pattern which is shown in Fig. 11 (a) and (b) represents a typical erosion attack on EB-PVD TBCs showing near surface cracking [31, 32]. The cracks stop at column boundaries and a number of neighbouring columns need to fracture before material is lost.

GZO has been extensively studied as an alternative TBC material to the standard 7YSZ in the literature due to its high thermal stability, low thermal conductivity, large coefficient of thermal expansion and reduced sintering at high temperature [33, 34]. GZO has shown a good resistance to VA/CMAS attack by forming a dense reaction layer consisting of an apatite phase which suppresses the infiltration into the inter-columnar gaps [11, 35]. However, its durability against real volcanic ash was never tested in a real engine atmosphere which was executed in this study. The GZO coated blisk was found to be more affected and susceptible to damage and the complete suction side has lost its ceramic coating (see Fig. 13 (a)). The damage is mainly believed to be caused by erosion as no VA infiltration or reaction with the GZO was observed (see Fig. 13 (c)&(d)). A different kind of erosion was observed on the

pressure side of the GZO blisk, where a significant local loss of the coating occurred which can penetrate to the substrate accompanied by deformation of the coating as shown in Fig. 13 (d). These type of damage correlates well to the compaction modus (FOD Mode 2) or FOD Mode 3 [31]. This type of damage can be caused by large particles travelling at low velocities or smaller particles at higher velocities. As the cold parts such as compressor blades were found to be eroded, these metallic particles would also fly through the combustor chamber and may additionally cause this kind of damage. At some parts re-deposition of VA on the metal surface after TBC removal is evident; see Fig. 13 (b). It is well known from the literature that the GZO coating has a lower toughness than 7YSZ which results in a significant reduction in the erosion performance [34, 36]. This effect is reflected here as well where erosion is believed to be the primary source for TBC failure in this study and the lower erosion resistance of GZO coating was caused by its cubic or ordered pyrochlore structure.

In essence, the main TBC failure mechanism of the described tests was erosion, accompanied by accumulation of volcanic ash that sticked to the surface of the TBC. Infiltration of VA within the TBCs could not be observed with the present test conditions. Therefore, a new design of combustor chamber and blisk is being currently developed with a higher TBC surface temperature so that the VA infiltration/reaction based damage of TBCs can be also assessed.

5. Conclusions:

A test apparatus has been constructed and successfully tested to simulate the degradation of components in a realistic micro aero-engine under volcanic ash (VA) containing atmospheres. A complete TBC system of either 7YSZ or GZO has been coated on several blisks by EB-PVD. The following conclusion can be drawn.

1. The constructed setup simulates the real aero-engine atmosphere and allows testing the effects of volcanic ash accumulation on the life time of TBCs in the regime of long time damage/unsafe operation zones according to the Rolls-Royce safe-to-fly chart.
2. Melting and deposition/sticking of volcanic ash particles on the TBC coated blisks was clearly observed with the setup. More volcanic ash deposition was observed on the leading edge compared to the trailing edge. Particles within the size range of 1-10 µm are more susceptible to melting and can also by pass the blades of the blisk without being deposited on turbine components, while larger particles did not melt or stay in semi molten state with sharp edges.
3. Since the TBC surface temperature was too low with the current setup, no volcanic ash infiltration into the TBC coatings was observed. Instead, many parts such as compressor blades, combustor liners, exhaust nozzles and the TBC coated blisks have undergone severe erosion.
4. Erosion related damage mechanisms such as near-surface cracking were observed in the 7YSZ coated blisk. Excessive damage was seen on the suction side compared to the pressure side of the blade.

An additional erosion mechanism namely compaction modus and FOD mode was observed in the GZO coating that was more eroded than the 7YSZ counterpart.

5. Overall, the 7YSZ has performed better than the GZO in the tested erosion/corrosion regime as the latter coating is tougher (t-phase) than the former (pyrochlore structure).

Acknowledgment

The authors express their gratitude to D. Peters and J. Brien for manufacture of TBCs on blisks, as well as A. Handwerk for providing technical support for test apparatus installation. Additionally, the authors thank R. Pubbysetty for his contribution in the metallography and electron microscopy related to the project and J.T. Gomez Chavez for XRD measurements of the ashes.

References:

1. M. G. Dunn, 'Operation of Gas Turbine Engines in an Environment Contaminated With Volcanic Ash', *Journal of Turbomachinery-Transactions of the ASME,* **134** (5) (2012).
2. H. N. Webster, D. J. Thomson, B. T. Johnson, I. P. C. Heard, K. Turnbull, F. Marenco, N. I. Kristiansen, J. Dorsey, A. Minikin, B. Weinzierl, U. Schumann, R. S. J. Sparks, S. C. Loughlin, M. C. Hort, S. J. Leadbetter, B. J. Devenish, A. J. Manning, C. S. Witham, J. M. Haywood, and B. W. Golding, 'Operational prediction of ash concentrations in the distal volcanic cloud from the 2010 Eyjafjallajokull eruption', *Journal of Geophysical Research-Atmospheres,* **117** (2012).
3. B. Weinzierl, D. Sauer, A. Minikin, O. Reitebuch, F. Dahlkotter, B. Mayer, C. Emde, I. Tegen, J. Gasteiger, A. Petzold, A. Veira, U. Kueppers, and U. Schumann, 'On the visibility of airborne volcanic ash and mineral dust from the pilot's perspective in flight', *Physics and Chemistry of the Earth,* **45-46** 87-102 (2012).
4. K. Turnbull, B. Johnson, F. Marenco, J. Haywood, A. Minikin, B. Weinzierl, H. Schlager, U. Schumann, S. Leadbetter, and A. Woolley, 'A case study of observations of volcanic ash from the Eyjafjallajokull eruption: 1. In situ airborne observations', *Journal of Geophysical Research-Atmospheres,* **117** (2012).
5. K. Weber, J. Eliasson, A. Vogel, C. Fischer, T. Pohl, G. van Haren, M. Meier, B. Grobety, and D. Dahmann, 'Airborne in-situ investigations of the Eyjafjallajokull volcanic ash plume on Iceland and over north-western Germany with light aircrafts and optical particle counters', *Atmospheric Environment,* **48** 9-21 (2012).
6. J. Eliasson, A. Palsson, and K. Weber, 'Monitoring ash clouds for aviation', *Nature,* **475** (7357) 455-455 (2011).
7. M. Guffanti, T. J. Casadevall, and K. Buddig, *'Encounters of aircraft with volcanic ash clouds; A compilation of known incidents, 1953-2009'*, U.S. Geological Survey Data Series 545, 1.0, 2010.
8. M. Guffanti, D. J. Schneider, K. L. Wallace, T. Hall, D. R. Bensimon, and L. J. Salinas, 'Aviation response to a widely dispersed volcanic ash and gas cloud from the August 2008 eruption of Kasatochi, Alaska, USA', *Journal of Geophysical Research-Atmospheres,* **115** (2010).
9. A. J. Prata, F. Dezitter, I. Davies, K. Weber, M. Birnfeld, D. Moriano, C. Bernardo, A. Vogel, G. S. Prata, T. A. Mather, H. E. Thomas, J. Cammas, and M. Weber, 'Artificial cloud test confirms volcanic ash detection using infrared spectral imaging', *Scientific Reports,* **6** (2016).
10. R. Darolia, 'Thermal barrier coatings technology: critical review, progress update, remaining challenges and prospects', *International Materials Reviews,* **58** (6) 315-348 (2013).
11. P. Mechnich, W. Braue, and D. J. Green, 'Volcanic Ash-Induced Decomposition of EB-PVD $Gd_2Zr_2O_7$Thermal Barrier Coatings to Gd-Oxyapatite, Zircon, and Gd,Fe-Zirconolite', *Journal of the American Ceramic Society,* **96** (6) 1958-1965 (2013).

12. R. J. Clarkson, E. J. Majewicz, and P. Mack, 'A re-evaluation of the 2010 quantitative understanding of the effects volcanic ash has on gas turbine engines', *Proceedings of the Institution of Mechanical Engineers, Part G: Journal of Aerospace Engineering,* (2016).
13. C. Taltavull, J. Dean, and T. W. Clyne, 'Adhesion of Volcanic Ash Particles under Controlled Conditions and Implications for Their Deposition in Gas Turbines', *Advanced Engineering Materials,* **18** (5) 803-813 (2016).
14. J. Dean, C. Taltavull, and T. W. Clyne, 'Influence of the composition and viscosity of volcanic ashes on their adhesion within gas turbine aeroengines', *Acta Materialia,* **109** 8-16 (2016).
15. W. J. Song, K. U. Hess, D. E. Damby, F. B. Wadsworth, Y. Lavallee, C. Cimarelli, and D. B. Dingwell, 'Fusion characteristics of volcanic ash relevant to aviation hazards', *Geophysical Research Letters,* **41** (7) 2326-2333 (2014).
16. W. J. Song, Y. Lavallee, K. U. Hess, U. Kueppers, C. Cimarelli, and D. B. Dingwell, 'Volcanic ash melting under conditions relevant to ash turbine interactions', *Nature Communications,* **7** (2016).
17. T. Steinke, D. Sebold, D. E. Mack, R. Vaßen, and D. Stöver, 'A novel test approach for plasma-sprayed coatings tested simultaneously under CMAS and thermal gradient cycling conditions', *Surface and Coatings Technology,* **205** (7) 2287-2295 (2010).
18. R. W. Jackson, E. M. Zaleski, D. L. Poerschke, B. T. Hazel, M. R. Begley, and C. G. Levi, 'Interaction of molten silicates with thermal barrier coatings under temperature gradients', *Acta Materialia,* **89** 396-407 (2015).
19. R. Naraparaju, U. Schulz, P. Mechnich, P. Döbber, and F. Seidel, 'Degradation study of 7wt.% yttria stabilised zirconia (7YSZ) thermal barrier coatings on aero-engine combustion chamber parts due to infiltration by different CaO–MgO–Al_2O_3–SiO_2 variants', *Surface and Coatings Technology,* **260** 73-81 (2014).
20. G. Warwick, 'NASA's Ash Trials: Engine Survives, provides Insight', *Aviation Week & Space Technology, Penton Media, New York, USA, 2015.*
21. M. Shinozaki, K. A. Roberts, B. van de Goor, and T. W. Clyne, 'Deposition of Ingested Volcanic Ash on Surfaces in the Turbine of a Small Jet Engine', *Advanced Engineering Materials,* **15** (10) 986-994 (2013).
22. C. Giehl, R. A. Brooker, H. Marxer, and M. Nowak, 'An experimental simulation of volcanic ash deposition in gas turbines and implications for ject engine safety', *Chemical Geology,* (2016).
23. T. J. Grindle and F. W. Burcham, '*Engine damage to a NASA DC-8-72 airplane from a high-altitude encounter with a diffuse volcanic ash cloud.*', N.t. report, NASA/TM-2003-212030, 2003.
24. N. I. Kristiansen, A. J. Prata, A. Stohl, and S. A. Carn, 'Stratospheric volcanic ash emissions fromthe 13 February 2014 Kelut eruption', *Geophysical Research Letters,* **42** (2) 588-596 (2015).
25. A. Yañez Gonzalez, C. C. Pilgrim, J. P. Feist, P. Y. Sollazzo, F. Beyrau, and A. L. Heyes, 'On-Line Temperature Measurement Inside a Thermal Barrier Sensor Coating During Engine Operation', *Journal of Turbomachinery,* **137** (10) 101004 (2015).
26. R. G. Wellman and J. R. Nicholls, 'Erosion, corrosion and erosion-corrosion of EB PVD thermal barrier coatings', *Tribology International,* **41** (7) 657-662 (2008).
27. P. Mechnich, W. Braue, and U. Schulz, 'High-Temperature Corrosion of EB-PVD Yttria Partially Stabilized Zirconia Thermal Barrier Coatings with an Artificial Volcanic Ash Overlay', *Journal of the American Ceramic Society,* **94** (3) 925-931 (2011).
28. W. Braue, P. Mechnich, and D. J. Green, 'Recession of an EB-PVDYSZ Coated Turbine Blade by $CaSO_4$ and Fe, Ti-Rich CMAS-Type Deposits', *Journal of the American Ceramic Society,* **94** (12) 4483-4489 (2011).
29. A. Hamed, W. Tabakoff, and R. Wenglarz, 'Erosion and deposition in turbomachinery', *Journal of Propulsion and Power,* **22** (2) 350-360 (2006).
30. T. J. Uihlein and U. Großmann. *Vergleichende Messungen Zum Einfluss Von Vulkanasche Und Sand Auf Verdichterwerkstoffe*. *Deutscher Luft- und Raumfahrtkongress* Bremen, 2011.

31. R. G. Wellman and J. R. Nicholls, 'A review of the erosion of thermal barrier coatings', *Journal of Physics D-Applied Physics*, **40** (16) R293-R305 (2007).
32. R. G. Wellman and J. R. Nicholls, 'The effect of TBC morphology on the erosion rate of EB PVD TBCs', *Wear*, **258** (1-4) 349-356 (2005).
33. C. G. Levi, 'Emerging materials and processes for thermal barrier systems', *Current Opinion in Solid State & Materials Science*, **8** (1) 77-91 (2004).
34. M. P. Schmitt, A. K. Rai, R. Bhattacharya, D. M. Zhu, and D. E. Wolfe, '"Multilayer thermal barrier coating (TBC) architectures utilizing rare earth doped YSZ and rare earth pyrochlores"', *Surface & Coatings Technology*, **251** 56-63 (2014).
35. S. Krämer, J. Yang, and C. G. Levi, 'Infiltration-Inhibiting Reaction of Gadolinium Zirconate Thermal Barrier Coatings with CMAS Melts', *Journal of the American Ceramic Society*, **91** (2) 576-583 (2008).
36. D. E. Wolfe, M. P. Schmitt, D. Zhu, K. R. Amarendra, and R. Bhattacharya. *Multilayered thermal barrier coating architectures for high temperature applications*. *36th Interntional Conference On Adavanced Ceramics And Composites*, Daytona Beach, USA, Wiley,2012.

Table 1: Chemical composition in wt.% of the VA particles obtained from EDS analysis (error lies in the range of maximum 5%).

Na	Mg	Al	Si	P	Cl	K	Ca	Ti	Fe
5.1	1.5	11.3	69.5	3.1	1	4.2	2.1	0.3	4.3

Figures:

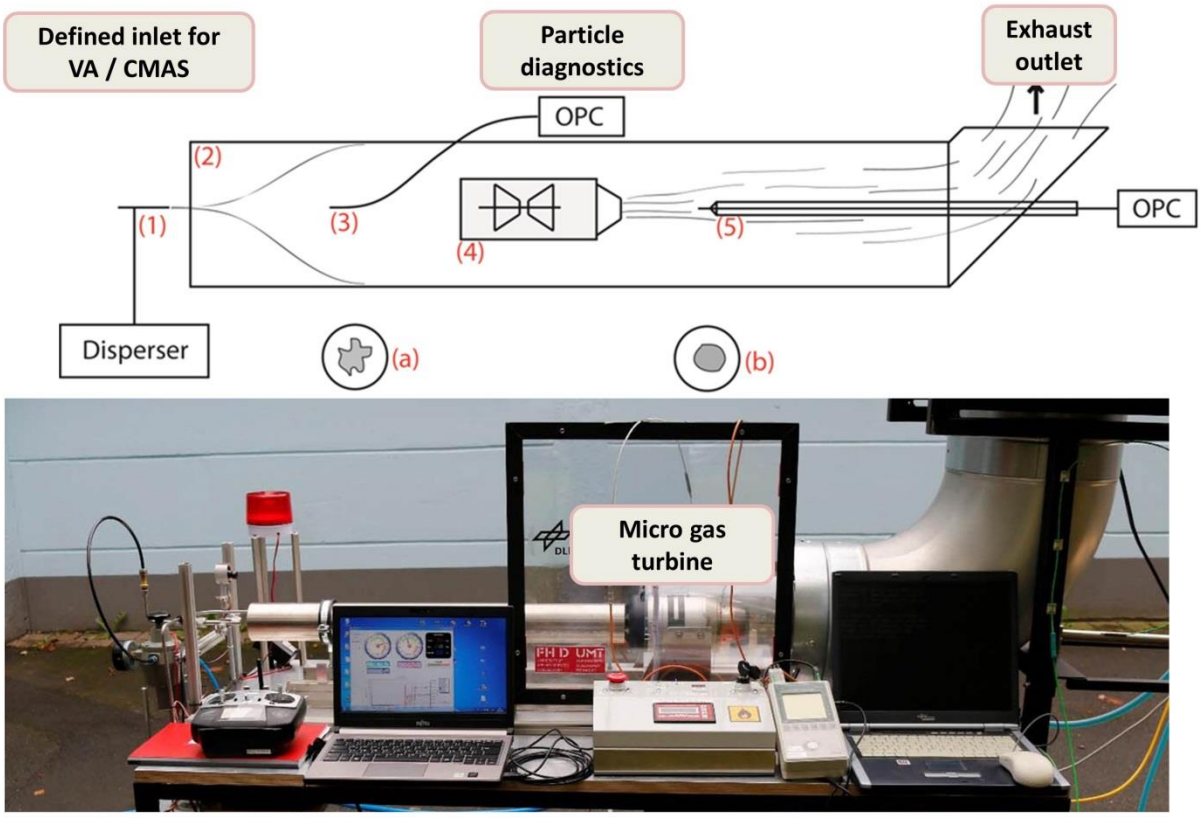

Figure 1: A schematic diagram representing the experimental set up used in this study.

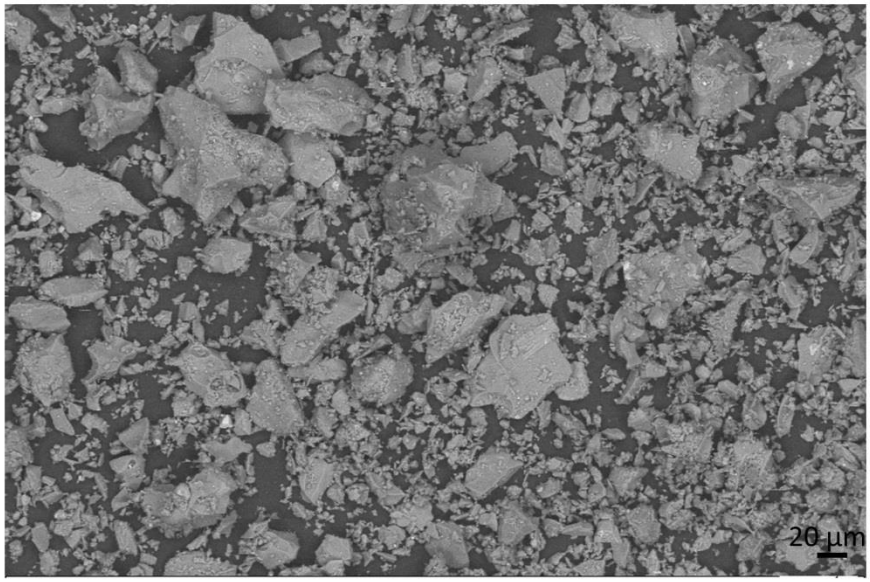

Figure 2: SEM micrograph of the VA particles used in this study (note the sharp edges of the particles).

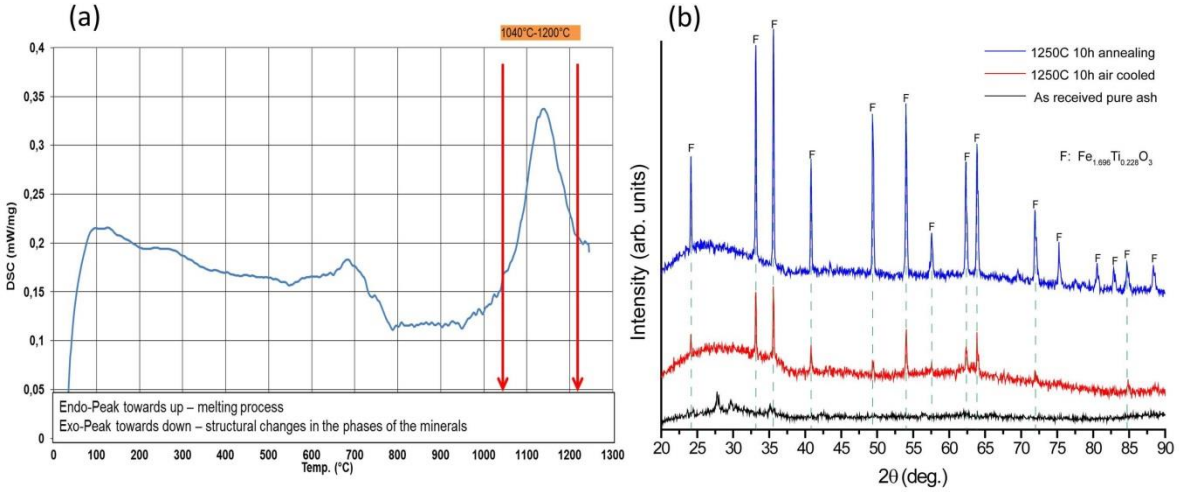

Figure 3: (a) DSC curve of Eyjafjallajökull volcanic ash and (b) XRD of as collected, heat treated volcanic ash.

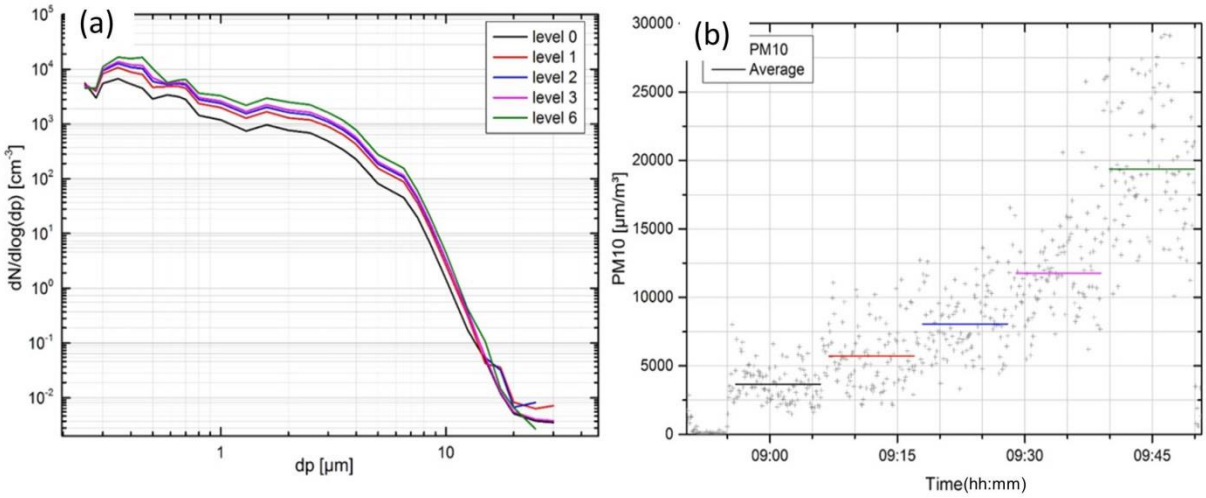

Figure 4: (a) particle size distribution measured by OPC system in front of the engine and (b) concentration of the ash in the air flow with respect to the disperser level settings for volcanic ash in the 1 to 10 µm size range.

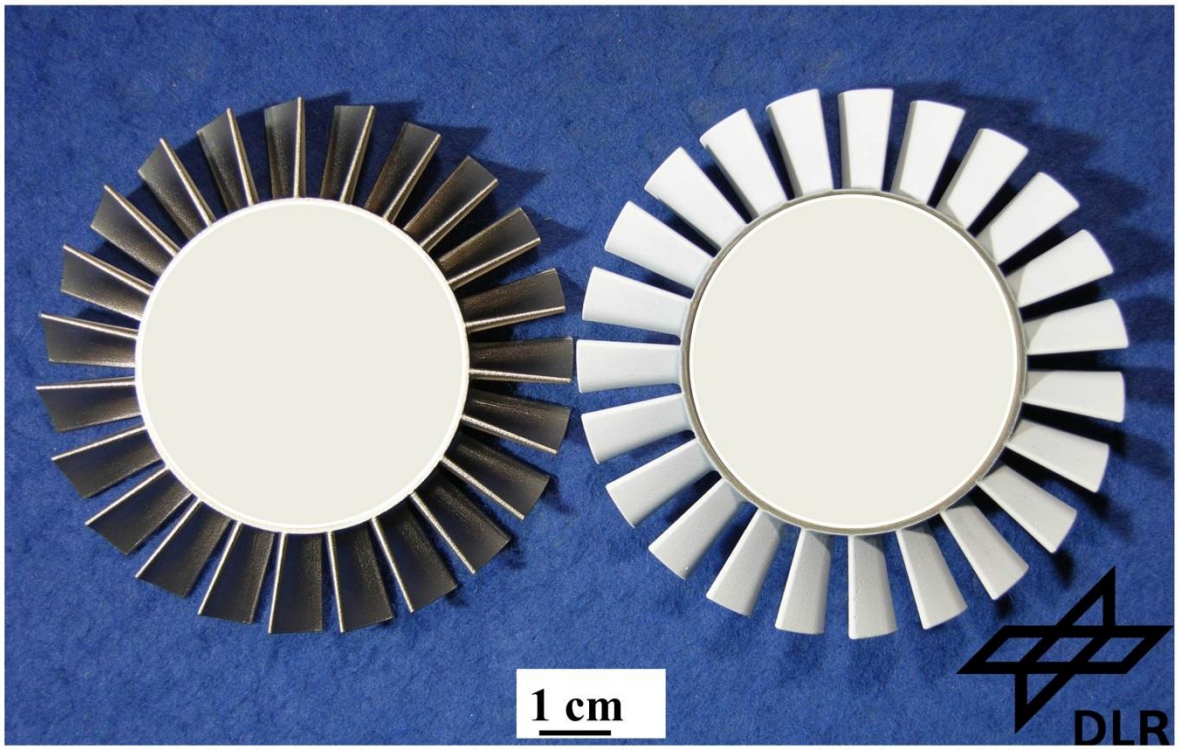

Figure 5: Photographs of the un-coated (left) and 7YSZ coated (right) blisks.

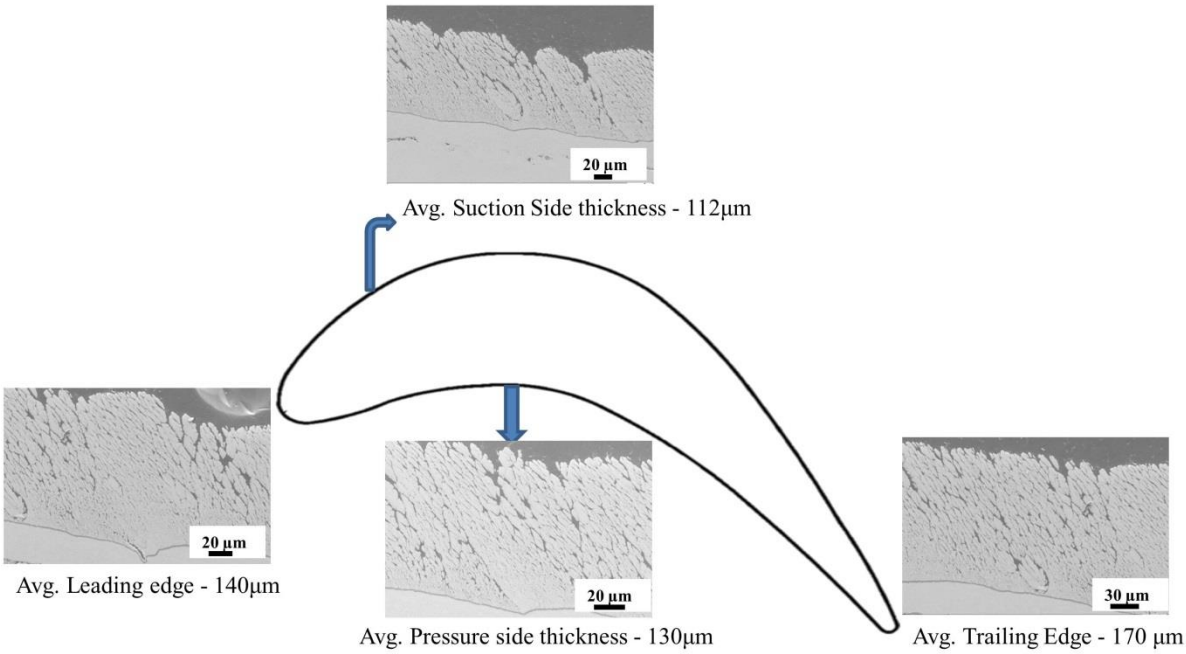

Figure 6: SEM images in cross section of the 7YSZ coating applied on different sections of the blade. Numbers give the average thickness of the TBC in the indicated region.

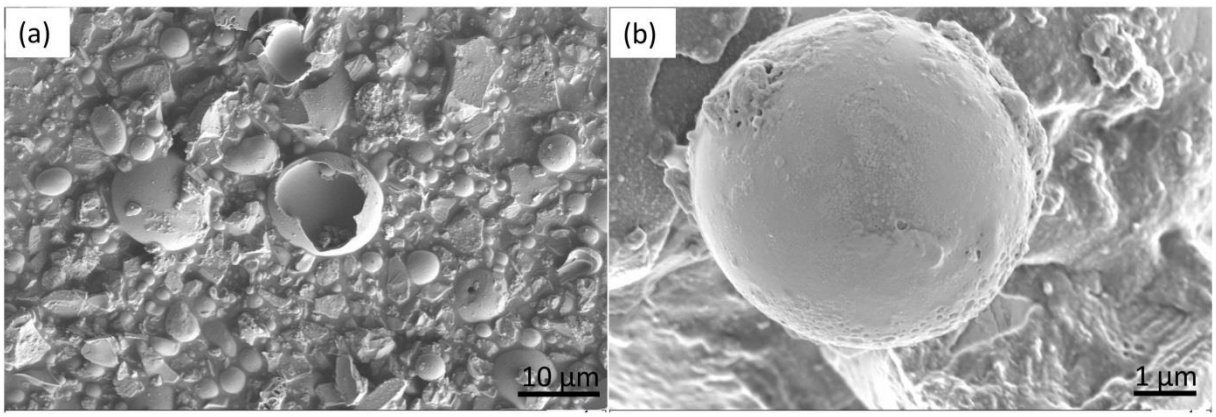

Figure 7: SEM micrographs of the collected VA particles in the exhaust. (a) Collected VA particles and (b) a high magnification image of a spherical VA particle.

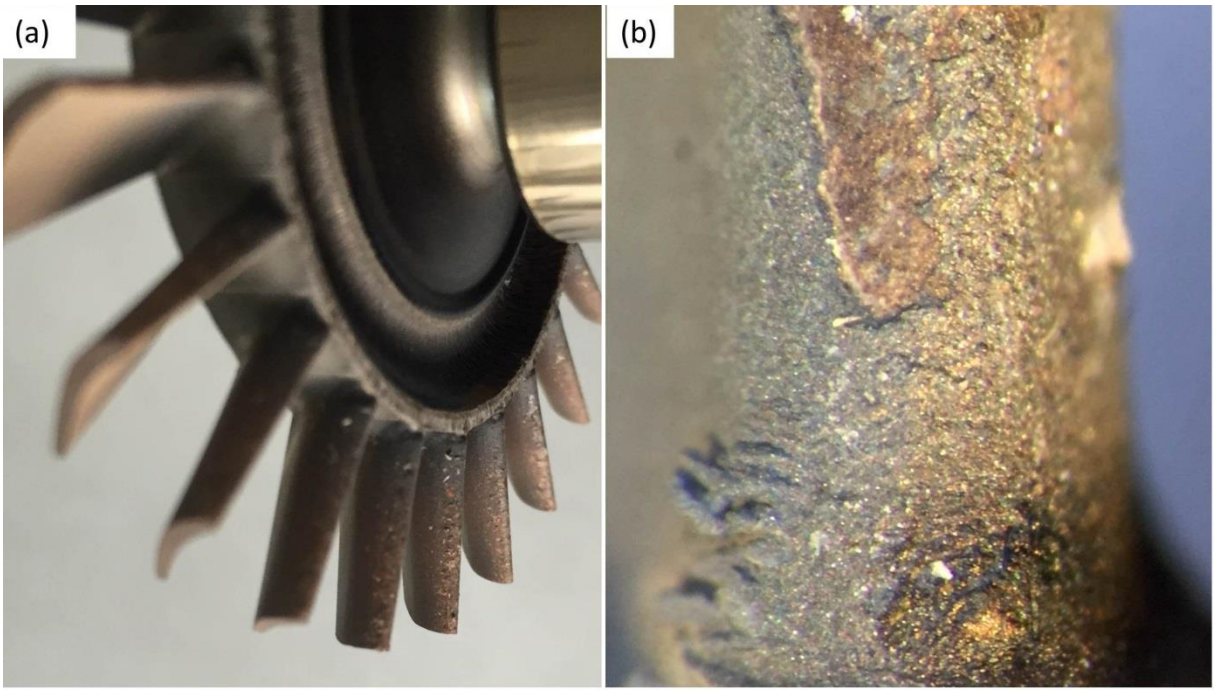

Figure 8: (a) Photograph of the tested blade having only the bond coat on top, containing VA deposit and (b) high magnification photograph showing deposits.

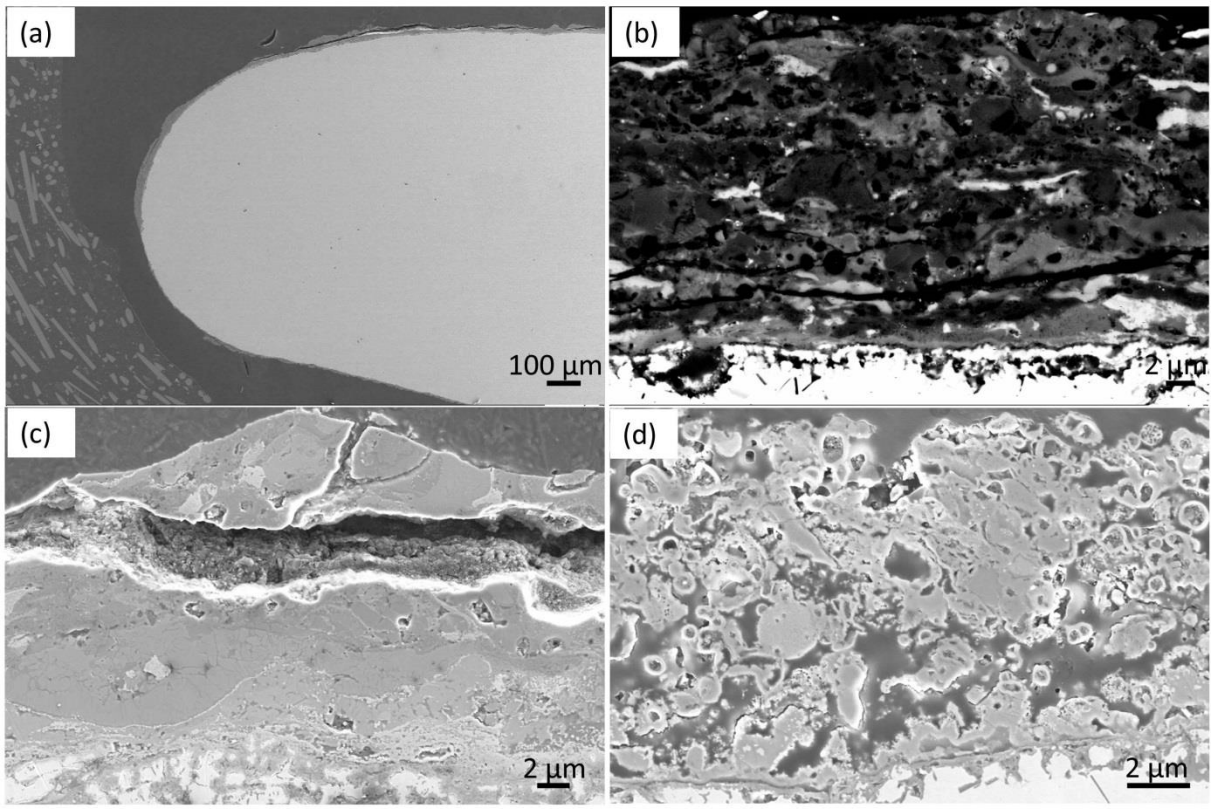

Figure 9: (a) SEM micrograph of the leading edge showing both the pressure and suction sides of a blade, (b) BSE image of VA deposit on top of the bond coat on the leading edge (c) VA on the suction side and (d) VA on the pressure side.

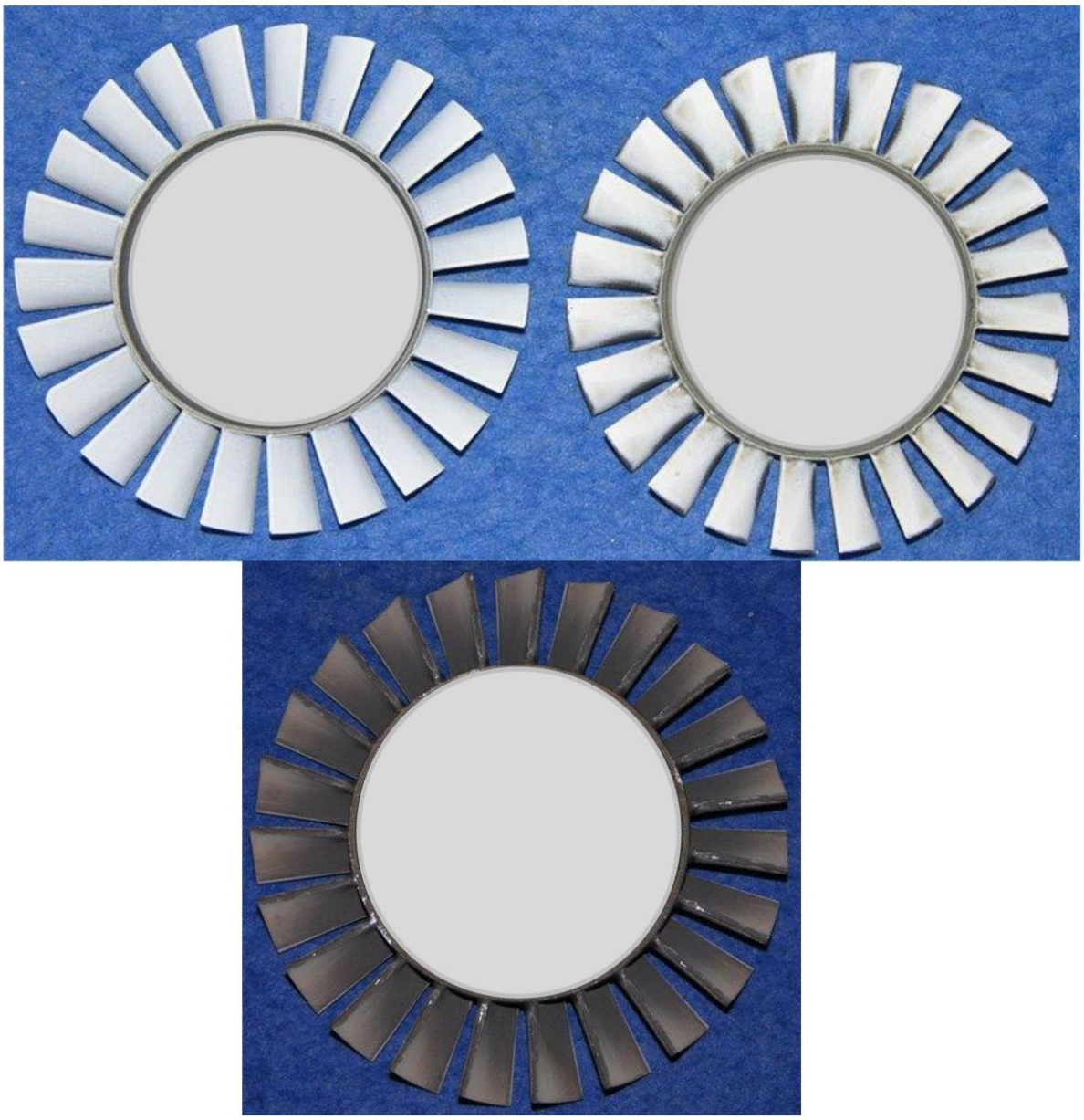

Figure 10: Photographs of the suction side of the 7YSZ blisk before (top left) and after the test run (top right) and pressure side (bottom) of the blisk after the test run.

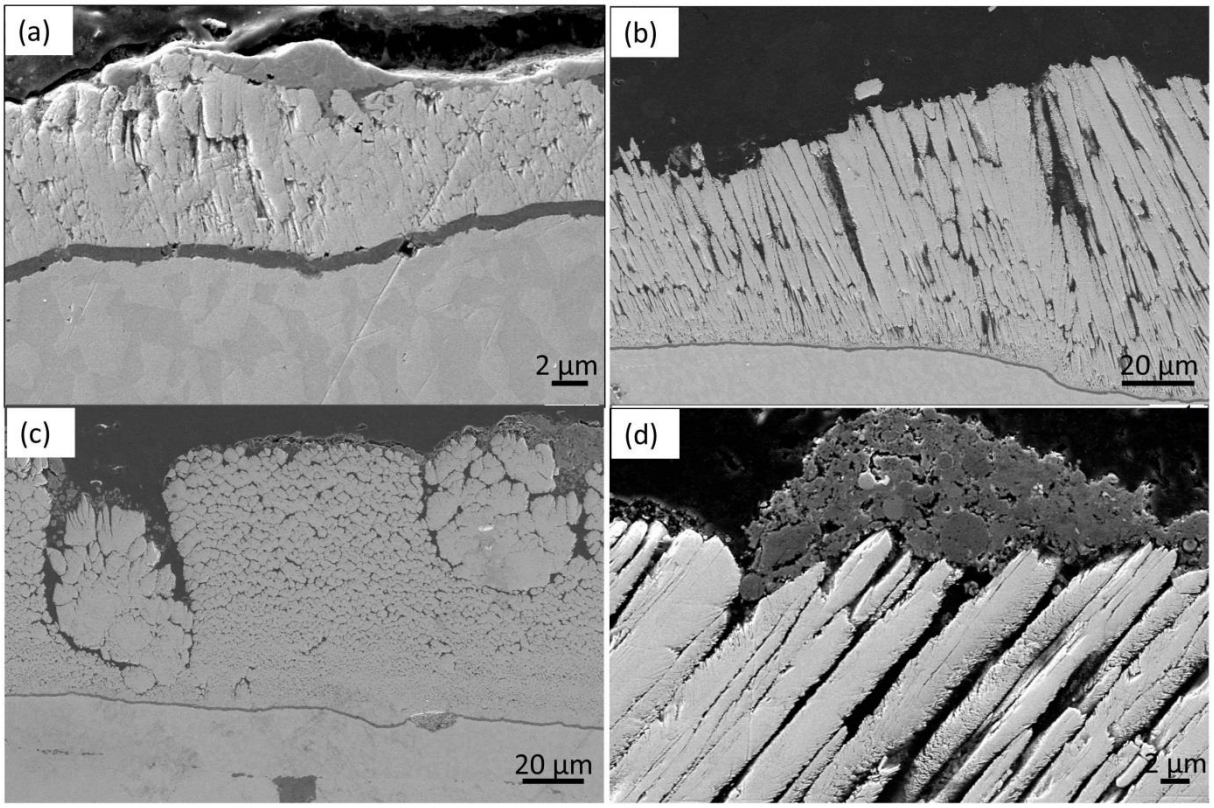

Figure 11: (a) & (b) Suction side of the 7YSZ blade in different cutting directions and (c) & (d) Pressure side.

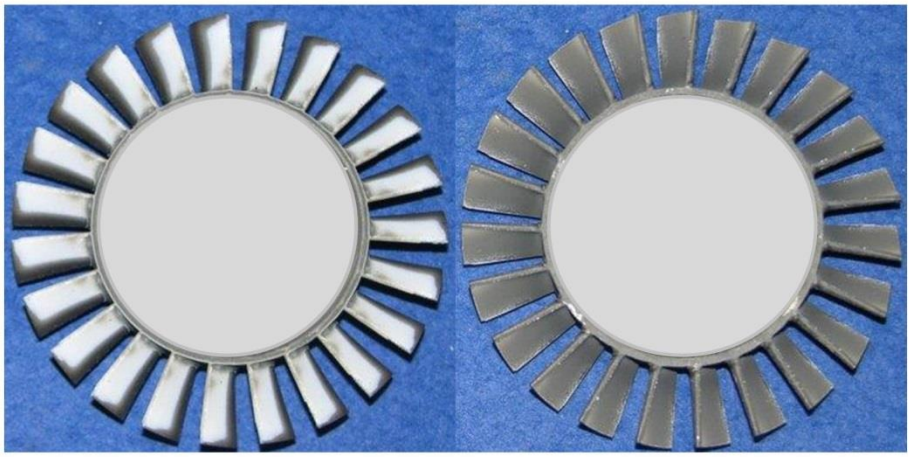

Figure 12: Photograph of the GZO coated blisk on suction (left) and on pressure (right) side after the test run..

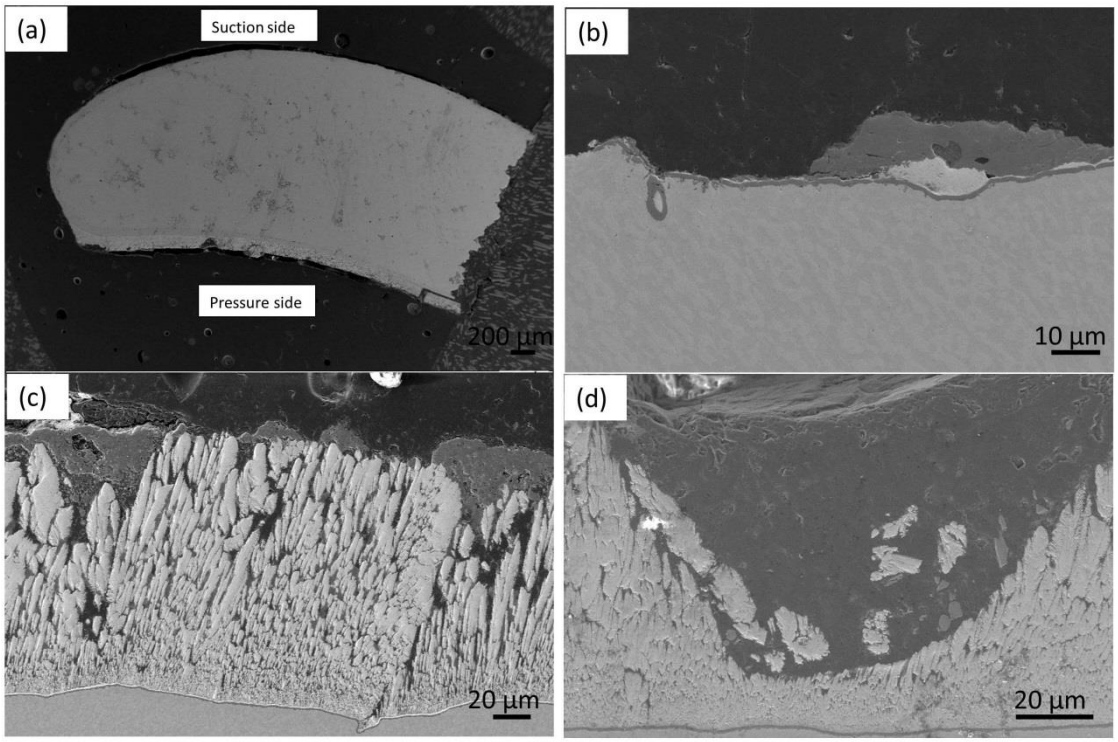

Figure 13: GZO blade with suction side (a)&(b) and pressure sides (c) & (d).

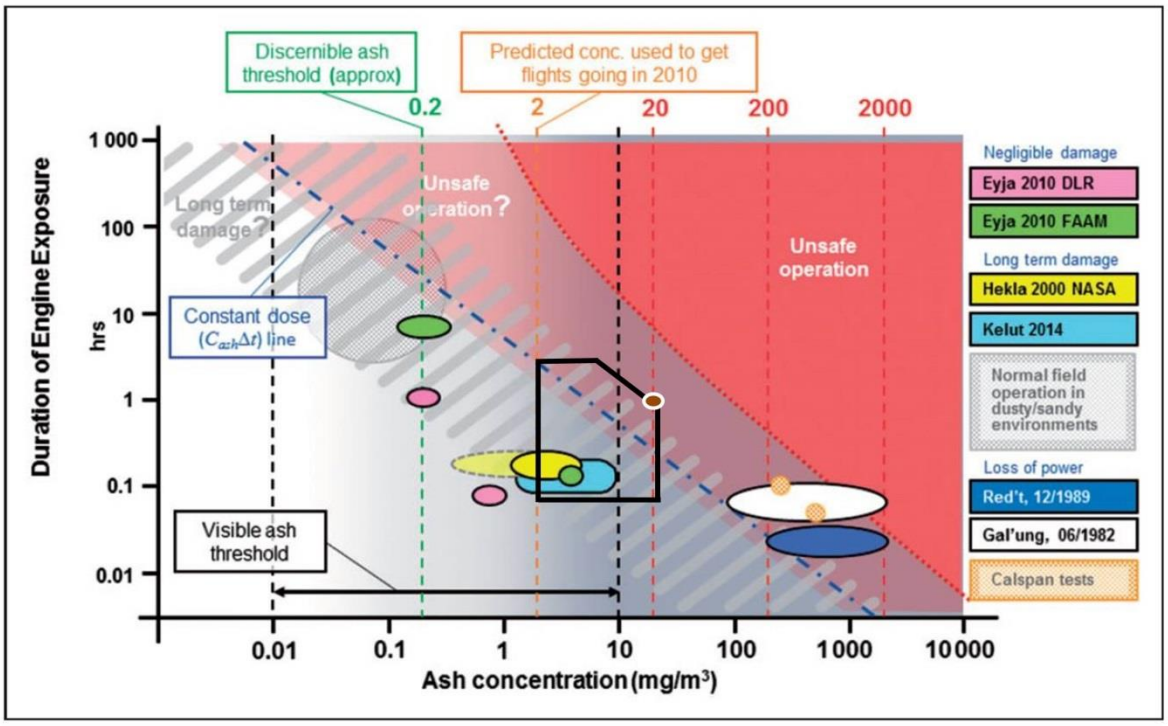

Figure 14: Duration of exposure against ash concentration chart with present test apparatus capability window added [9].